

Linear Feature Based Matching of Stereo SPOT Satellite Images

Nigel Butler
Research Student
School of Surveying
University of New South Wales
PO Box 1, Kensington
Sydney, NSW, 2033
Australia
nigel@spectrum.cs.unsw.oz.au

Commission IV

Abstract

A new technique utilizing Feature-Based Matching of stereo SPOT satellite images to derive Digital Elevation Models (DEMs) is presented. DEMs were derived by extracting and then matching linear features from stereo image pairs. The features were extracted by convolving the images with 2x2 pixel windows and grouping the image pixels upon similar gradient orientation. A pair of 8 mutually exclusive binary images are produced and are labelled via a connected-components algorithm. Lines are fitted to regions and parameters calculated providing a rich set of attributes, which are then used to match corresponding features in the stereo images. Heights are derived from these matches and manually checked, with accuracies approaching the pixel level. These points are also triangulated into a network of nearest-neighbors. The network is interpolated onto a regular grid and one of the images of the stereo pair may be draped over the generated DEM.

Key Words: Feature Extraction, Image Matching, Stereoscopic, SPOT, DEM.

1 Introduction

Feature Based Matching of stereo satellite images was performed to obtain a Digital Elevation Model (DEM) by extracting and then matching linear features from stereo pairs. In recent years the focus on the solution to automated stereo matching has shifted from gray-level correlation to feature-based matching (Greenfeld and Schenk, 1989). Feature and area based image matching has been tested and compared with hybrid approaches (Brockelbank and Tam, 1991). Very few projects attempting to assess the feasibility of using SPOT stereodata as a source of height information have been carried out and few results have been presented (Theodossiou and Dowman, 1990).

The technique may be applied to images acquired both in the near and far range, however this paper is concerned with the far range. The stereo analysis problem as in previous treatments (Barnard and Fishler, 1982, Medioni and Nevatia, 1985) may be broken into the following steps:

- image acquisition,
- camera modelling,

- feature acquisition,
- image matching,
- distance (depth) determination and interpolation.

Extensive work has already been completed in the camera modelling of the SPOT stereo system and the Sydney images in particular. The collinearity equations, the ephemeris data from the header of the SPOT images and a set of known control points were used to specify the camera model. Precision of computation of object coordinates have been shown to be of the order of 5-10 meters in planimetry and height coordinates depending on the precision of the ground control points (Trinder *et al.*, 1988).

The focus of this project is on the last three stages of the list above. Figure 1 shows the image matching process followed.

2 Image Acquisition

Since the launch of SPOT-1 on the 22nd February 1986, the production of topographic maps from space on an operational basis is now a possibility. SPOT acquires high resolution imagery of almost all of the earth's surface and on the basis of coverage per single image, its imagery is cheaper than aerial photography (Trinder *et al.*, 1988).

The test stereo pair of SPOT images consists of scenes of Sydney and its metropolitan area. One was imaged on the 22nd November 1986 with a *left* incidence angle of 30.1° and the other on the 12th October 1986 with a *right* incidence angle of 21.3° (i.e. six weeks between dates of acquisition). The *Base to Height* (B/H) ratio of the pair was therefore 0.97.

Different stereo applications often involve different kinds of scenes. Perhaps the most significant and widely recognized difference in scene domains is between scenes containing cultural features such as buildings and roads, and those containing only natural objects and surfaces, such as mountains, flat or 'rolling' terrain, foliage, and water. Industrial applications, on the other hand, tend to involve artificial, cultural objects exclusively. Cultural features present special problems. For example, periodic structures such as the windows of buildings and road grids can confuse a stereo system.

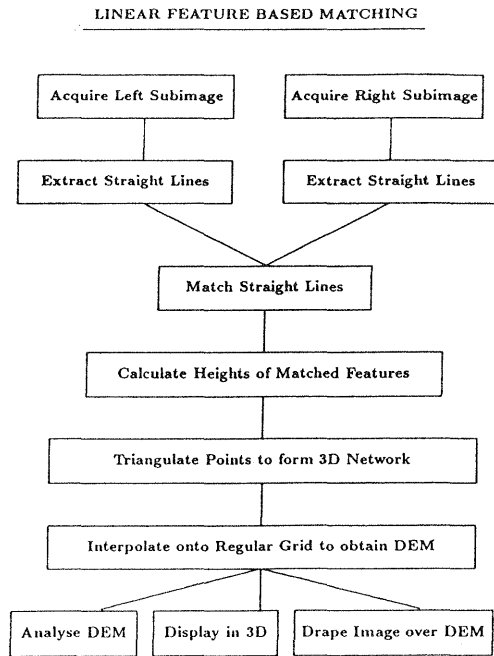


Figure 1: Linear feature-based matching method.

The relative abundance of occlusion edges in a city scene can also cause problems because large portions of the images may be unmatched. The only major occlusion in the images considered occurs at the cliffs on the coast.

The complexity of the scene domain in stereo applications is affected by:

- occlusion,
- artificial objects (straight edges, flat surfaces),
- smoothly textured areas,
- areas containing repetitive structures (Barnard and Fishler, 1982).

In addition to these factors, satellite stereo images contain distortion due to earth curvature and although both images were obtained at approximately the same time of the day, the satellite was on the 'same' side as the sun for the east (right) image and on the 'other' side for the west (left) image. Hence, the image brightness and edge contrast varies between images.

The whole of the left image (6000 by 6000 pixels) was subdivided into 500 by 500 pixel subimages. Where each left subimage was compared with the corresponding right subimage. The pixel coordinates of the center of the right subimage may be approximated from the camera model and an initial estimate of the height of the terrain. The accuracy of this height estimate was improved by interpolation from the set of known matched control points and hence depends on proximity to the control points. Once a point from each image is known to match, the height may be determined from the camera model.

3 Camera Modelling

The standard photogrammetric collinearity equations are not applicable to linear push broom imagery. This is because in a linear array image, only one line is imaged at any one instant of exposure. Hence a separate set of collinearity equations are required for each line of the image.

Individual SPOT scenes are arbitrarily selected segments of the inherently continuous imagery. In contrast to frame cameras, which preserve the same orientation of the three-dimensional bundle of imaging rays for the whole frame, the

- spatial position and
- orientation

of the imaging sensor is continually changing along the orbit and the imaging geometry becomes dynamic and time-dependent (Kratky, 1989).

Taking the image x-axis to be in the direction parallel to the epipolar plane (as in conventional photogrammetry), it can be noted that the projective relationship exists only in the x-z plane of the image space (Trinder *et al.*, 1988).

A set of 31 control points known to match was also included in the model to increase accuracy. Before these points were added, the location of a pixel in the right image may be predicted to within 600 meters given the left image coordinate and a reliable estimate of the ground height. The addition of control points allow sub-pixel accuracy given the correct height.

In dealing with satellite imagery, there are several possible coordinate systems which may be selected. A local space rectangular coordinate system was chosen with the appropriate corrections applied for earth curvature, and the difference between local space rectangular and grid coordinate system (e.g. UTM). The coordinates for the satellites position are used to provide approximations for the solution of ground coordinates rather than to pinpoint the location of the satellite at the time of the imagery. The local space rectangular coordinate system is thus the best choice for both the solution of the orientation parameters and also for the real-time equations used for plotting (Trinder *et al.*, 1988).

4 Feature Acquisition

Techniques used for stereo matching may be broadly divided into area-based and feature-based matching. For area-based matching, a local match for an area is found by searching in the other image for the best match defined by a cross-correlation measure, sum of absolute differences of pixel intensity or other similar measures (Medioni and Nevatia, 1985).

All systems based on area-correlation suffer from the following limitations:

- They require the presence of a detectable texture within each correlation window, therefore they tend to fail in featureless or repetitive environments.
- They tend to be confused by the presence of a surface discontinuity in a correlation window.

- They are sensitive to absolute intensity, contrast, and illumination.
- They get confused in rapidly changing depth fields (eg vegetation).

For these reasons, the existing systems, especially the ones used in automatic cartography, require the intervention of human operators to guide them and correct them (Medioni and Nevatia, 1985).

As feature matching necessarily leads to a sparse depth map only and tends to be confused in densely textured areas, feature matching should be regarded as complementary to, rather than as competing with, area-based matching (Hannah, 1989). The rest of the surface must be reconstructed by interpolation.

Some advantages of feature-based systems are:

- They are faster than area-based methods, because there are fewer points (features) to consider;
- The match is more accurate as edges may be located with sub-pixel precision;
- They are less sensitive to photometric variations, since they represent geometric properties of a scene (Medioni and Nevatia, 1985).

Some other advantages noticed while observing matched lines overlaid on the image pairs was the ability of some feature pairs to be located correctly, although the surrounding features might vary greatly either due to temporal change or reflectance characteristics due to the geometry of the system. Also, many elongated features extracted through the grouping mechanism would be larger than the pixel windows used in area-based techniques.

4.1 Edge Pixel Determination

Linear features were extracted by convolving the images with 2×2 pixel windows and grouping the image pixels upon similar gradient orientation. The pixels are grouped into so-called *line-support regions* (LSR). The LSR refers to a single change in image intensity in a direction normal to the orientation of the edge. A pair of 8 mutually exclusive binary images are produced according to the *Overlapping Partitions* technique (Burns *et al.*, 1986).

This technique proved to be extremely useful in extracting lines of any orientation by grouping pixels under two separate partitions of the 0° - 360° gradient orientation spectrum. The critical problem of this approach is the merging of the two representations in such a way that a single line in the image is principally associated with a single LSR. The regions considered best are the ones which provide an interpretation of the line which is the longest (Burns *et al.*, 1986).

4.2 Labelling Binary Images

The pixels were grouped on gradient orientation by labelling binary images using a modified method of Winston's technique (Winston and Horn, 1984). Each binary image is composed of thousands of components (or regions). Lines are fitted to these regions and attributes determined (e.g. location, orientation, length, contrast, width and straightness). The location of straight lines within an image may be determined to sub-pixel accuracy.

4.3 Fitting Lines to Regions

If the intensity image of an edge and its surrounds is thought of as a 3-dimensional surface with x and y as the column and row of the image, respectively, and z as the intensity of the image then this produces what is termed an intensity surface. In these terms the line extracted refers to a step, that is a single change in intensity. The line extracted does not refer to an intensity surface which forms a ridge for which there is no distinct location for the boundaries on either side of the ridge. In Burns view these narrow linear image events will have a width formed by two locally parallel lines of opposite contrast (anti-parallel vectors).

Burns approximates the intensity surface associated with each LSR with a planar surface. Straight lines are then extracted by intersecting this fitted plane with a horizontal plane representing the average intensity of the region weighted by a local gradient magnitude.

The method used here fitted the LSR with its axis of least inertia, also weighted by local gradient magnitude, using the Hough parameterization of the line. McIntosh and Mutch's method (McIntosh and Mutch, 1988), also uses moments of inertia, however, edge pixels were not weighted.

The axis of least inertia passes through the centroid of the area. Least squared error line fitting with this form of line equation (as opposed to slope-intercept) minimizes errors perpendicular to the line (as opposed to those perpendicular to one of the coordinate axes) (Ballard and Brown, 1982).

Deriving the orientation of the axis requires *least-square* fitting by minimizing the sum of the squares of the distances of the pixels from the line using the *Hough* (ρ, θ) parameterization of the line.

Figure 2 shows a frequency histogram of line lengths for a subimage with center pixel coordinates (2750,3250) with respect to the main image. The frequencies for lengths up to and including 1 and 2 were omitted due to their very large number which may be partly attributed to noise. The thresholds placed on line length in the program provides a good filter on noise and poor quality lines. The frequencies decline very rapidly for increasing line length.

4.4 Average Intensities

The average intensity of the whole subimage was determined before the gradient magnitude threshold and line length threshold were set. A lower threshold was used for the relatively dark, featureless subimages. A higher threshold for the brighter subimages with more densely spaced cultural (artificial) features. This serves the dual purpose of maximizing the information retrieved from the dark areas, while limiting the wealth of data to be analyzed from the high spatial-frequency areas.

A brief analysis of the relationship between subimage average intensity and the number of lines produced of various lengths was performed to ascertain whether any trends occurred. This was to limit if possible the volume of data produced in the city scenes, while at the same time maximize the data from the relatively dark and featureless subimages.

The frequency of lines with various length-ranges was displayed on a square root scale as the features are extracted

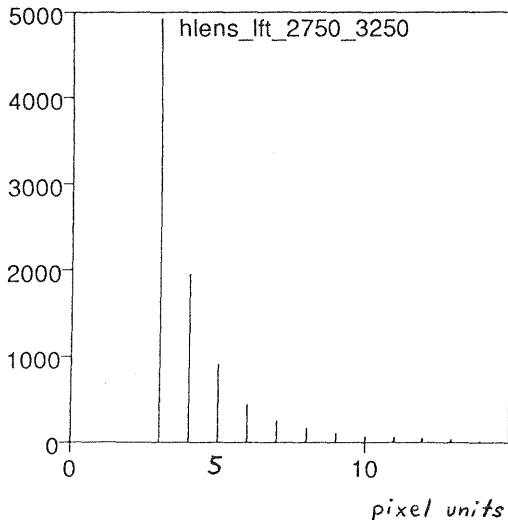


Figure 2: Frequency histogram of line lengths for typical subimage.

from two-dimensional images. Any increase in cultural activity is expressed by more features per unit area. This selection of scale was useful and a general trend was found which was used as a basis for adjusting threshold parameters.

It was found from graphs such as Figure 3 that the value on the y -axis of an x -value > 50 pixels is approximately the same as that of the next line above for an x -value < 50 pixels. That is, lines of shorter length may be included when dealing with darker subimages to produce a similar number of total lines with respect to the brighter subimages.

4.5 Remaining Line Attributes

All the line attributes to be extracted are: 1) orientation, 2) location, 3) length, 4) width, 5) contrast, 6) steepness, 7) dark edge and 8) light edge. A straightness attribute has been derived but has not been implemented during the matching stage.

The width being defined to be the area of the *line support* region divided by the length of the line. The light edge and dark edge values are the average of the lightest and darkest 10% of the pixels in the region, respectively. Contrast is the difference between the light and dark edge values (McIntosh and Mutch, 1988). Steepness of the intensity surface of the edge was the average gradient magnitude of the region in McIntosh and Mutch, but was evaluated here as the contrast divided by the width.

An additional parameter describing the shape was used as extra information for the matching. The straightness parameter was estimated by determining the longest line contained in the region and ratioing the distance of the centroid from this line over the length of the line.

4.6 Linking Lines

An optional step at this point is to link lines with similar attributes and a close pair of endpoints. In some cases

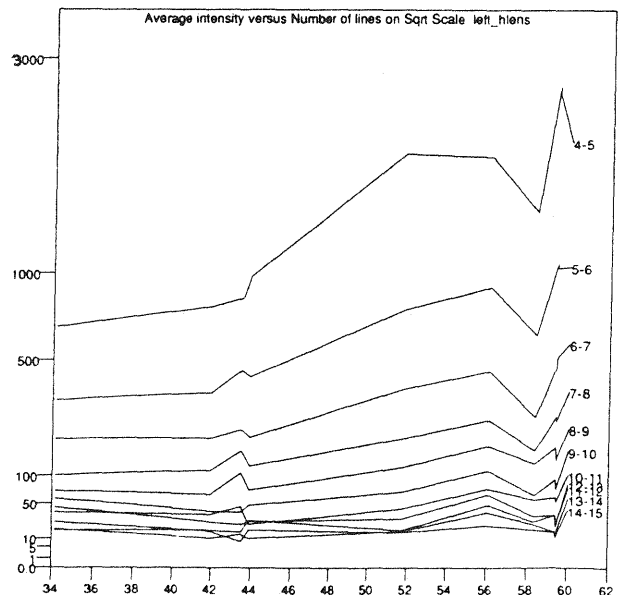


Figure 3: Average intensity versus number of lines produced for an East-West strip of left subimages. Note vertical axis has a square root scale. Each line represents the number of lines produced for a particular range of lengths.

this is important as a single long line in one image may correspond to two line segments in the other image and an opportunity for a match may be lost. However, the aim of the project is to obtain as many precisely located features as possible and over-linking of lines might reduce the density of points in the network after matching has been performed. In (Zhou *et al.*, 1989), lines are linked based on certain criteria and some are extended to meet at corners.

Line linking has been implemented, if endpoints from two lines are within 5 pixels, and if after the lines have been mapped into points in (ρ, θ) space using the Hough Transform their proximity is less than 2 units and the remaining parameters are similar then the lines were linked.

4.7 Filtering Lines

Lines are filtered as a final step in the extraction process. Lines with very short lengths may represent noise or texture and ignoring these lines allows removal of noise without resorting to preprocessing the image using digital image processing techniques. Short lines derived from regions of small area will have attributed to them a set of unreliable parameters. Width, steepness, contrast etc are all more representative the longer the line and the larger the region from which they were obtained.

Also, lines with near horizontal orientations are not good for matching as they are nearly parallel to the epipolar plane. If different portions of the same horizontal linear feature are extracted from each image of the stereo pair, then all parameters may be similar and the epipolar constraint satisfied but an incorrect height obtained.

Figures 4 and 5 show the result of extracting lines from

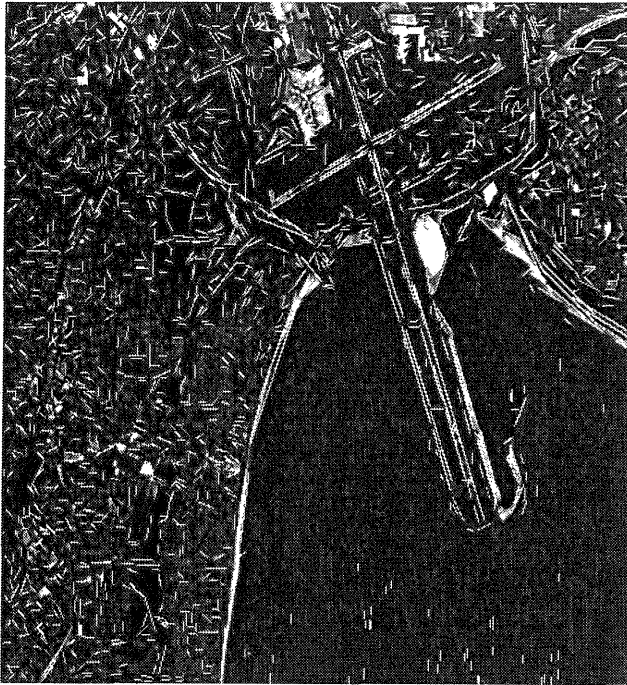


Figure 4: Extracted lines from left subimage of Sydney Airport region.



Figure 5: Extracted lines from right subimage of Sydney Airport region.

SPOT subimages over the Sydney Airport region. The average intensity of one subimage was approximately 46. Normally the images with lower average intensities are due to densely vegetated, relatively featureless areas, however, this image has low average intensity due to the presence of a large body of water. As a result, this image is considered relatively dark and so the gradient magnitude threshold, minimum length and region-area thresholds are kept low to allow more lines to be extracted. The actually threshold values used were:

$$\begin{aligned} \text{Gradient Magnitude} &= 6 \text{ grey scale/pixel} & (1) \\ \text{Length Minimum} &= 5 \text{ pixels} & (2) \\ \text{Area Minimum} &= 5 \text{ square pixels} & (3) \end{aligned}$$

The process of line extraction is performed on both images of each stereo pair. All line attributes from the left subimage are stored in one database file, and all from the right subimage are stored in a second file.

Certain lines from the left file are compared with certain lines from the right file depending upon various geometrical constraints and line pairs considered to match are determined, as explained in the following section.

5 Image Matching

Matching is generally recognized as the most difficult stage in stereo vision. Once straight lines are extracted from both images and attributes determined (eg location, orientation, length, contrast, width and straightness), a match function is defined which determines the strength of the similarity between a pair of lines. The location of

straight lines within an image may be determined to sub-pixel accuracy. Pairs which are a mutually best match, based on the match function and correspondence constraints (epipolar, continuity) are considered corresponding lines (McIntosh and Mutch, 1988).

With the continuing advance in computer memory and speed it is feasible to produce thousands of lines per subimage with arbitrarily strict filters on line quality (eg threshold on line length) during the extraction stage and arbitrarily strict matching criterion on match quality (eg large match function threshold). Due to the large number of features examined, a modified implementation of the matching algorithm in (McIntosh and Mutch, 1988) was required.

McIntosh and Mutch's algorithm for matching straight lines examines images of indoor scenes and industrial objects. This paper also uses Burns' method for the initial stage of extracting straight lines.

Features in *close range* environments differ from the *distant range* application under consideration with regard to the geometry and distortions in the satellite images. Also, each linear feature is more important and there is a greater possibility for occlusion of surfaces in the *close range*.

Nevertheless, the general matching principle of McIntosh and Mutch's algorithm has been adapted and has been found quite satisfactory. The matching algorithm finds corresponding pairs of lines on a pair of images based on a *match function*. This function combines a set of eight descriptive parameters of each line, which may be weighted according to their relative importance.

Corresponding lines are those which have the largest

match function values. Matching is performed in both directions (i.e. from image L to R , and from image R to L), and only lines which correspond in both directions are considered to be matched (McIntosh and Mutch, 1988). To reduce the number of line pairs analyzed and reduce execution time, constraints were placed on which lines in the right image were allowed to be compared to lines in the left image.

5.1 Continuity and Epipolar Constraints

The *disparity distance* was determined for each line pair by predicting where the centroid of a line in the left image would occur when mapped into the right image from the camera model and a height from the triangulated control-points. The distance, in right image coordinates, between this predicted position and the actual centroid of the line in the right image was a measure of the *disparity distance*.

The *continuity constraint* specifies that the disparity of a point will be similar to the disparity of nearby points. Although there is a slight rotation between the left and right images, it may be assumed that limited rotation takes place between corresponding lines.

As a further constraint related to the *epipolar plane* (as mentioned in the previous section), it is known that lines with near horizontal orientations are ineffective for matching as they are nearly parallel to the epipolar plane. Ideally, matching lines orthogonal to the *epipolar plane* are optimal for accurate height generation. Therefore, only lines making less than a certain acute angle with the vertical were used. That is:

$$\text{Acute Angle}(\text{Line}_L) \text{ with } y\text{-axis} < 70^\circ \quad (4)$$

$$\text{Acute Angle}(\text{Line}_R) \text{ with } y\text{-axis} < 70^\circ \quad (5)$$

Constraints were also placed on the difference in angles of the possible line pairs and also on the difference in lengths.

5.2 Match Function

For a given line pair, the match function measures the *similarity* of the eight parameters attributed to each line. Each parameter has a corresponding weight, with the sum of all the weights being 1.

$$\sum_{k=1}^8 W_k = 1 \quad (6)$$

where W_k = weight of the k th parameter.

Initially, a two-dimensional array of match values was defined for the similarity measure of each line from image L to each line from image R . However, a more efficient method of storage was found to accommodate the vast amounts of data in the distant range application. Each element in the array was the sum of the weighted similarity values for each parameter. The match function array was defined as:

$$M_{LR} = \sum_{k=1}^8 V_k W_k \quad (7)$$

where $L = 1, 2, \dots, M$, $R = 1, 2, \dots, N$, and M is the number of lines in set L (left lines) and N is the number of lines in set R (right lines) and V_k is the similarity measure

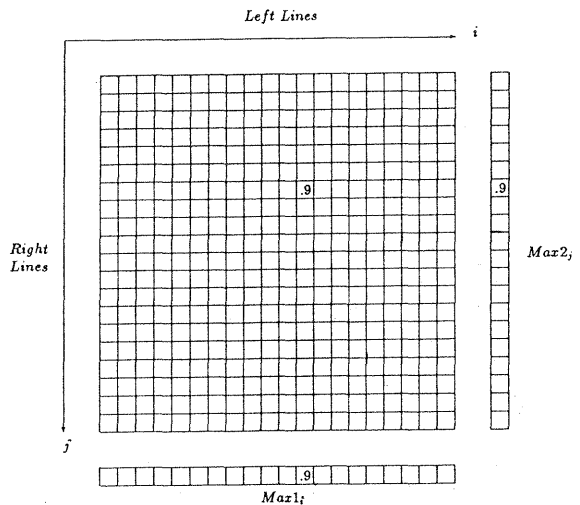


Figure 6: Two-dimensional array of match functions with one-dimensional projections of their maxima.

of the k th attribute of a line pair. A search for the best match for each line is then performed.

Two arrays are computed to determine the best match of each line from each image. These arrays are defined as:

$$MAX1_L = \max(M_{Lj}, j = 1, 2, \dots, N), \quad (8)$$

$$MAX2_R = \max(M_{iR}, i = 1, 2, \dots, M). \quad (9)$$

If line R from the right image is the best match to line L from the left image, and line L in the left image is the best match to line R in the right image, then L and R are a *mutually best match*. Then if the match function of L and R is greater than the predefined match threshold, lines L and R are considered a match (McIntosh and Mutch, 1988). That is,

$$\begin{aligned} &IF (MAX1_L \equiv MAX2_R) \text{ AND} \\ &(MAX1_L > MatchThreshold) \\ &THEN \text{ Correspond}(L, R) \end{aligned}$$

To avoid the need to store all the NM values of a two-dimensional array, M_{ij} , the one-dimensional *projection* of its maxima in both dimensions is stored, as shown in Figure 6. That is, $(N + M)$ values instead of NM .

5.3 Results

The height of the feature on the ground in Universal Transverse Mercator (UTM) coordinates may then be derived from the geometry and orientation of the satellite at the time of data acquisition.

Figure 7 shows the combined subimage triangulations in ENH coordinates. An obvious feature from this figure is the 9° rotation of the ground coordinate (UTM) system with respect to the SPOT sensor image coordinate system. This is due to SPOT's sun-synchronous polar orbit.

The sparseness of the triangulations in the South-East of the image is due to the dark, densely-vegetated, relatively featureless National Park. Gaps to the East are due to

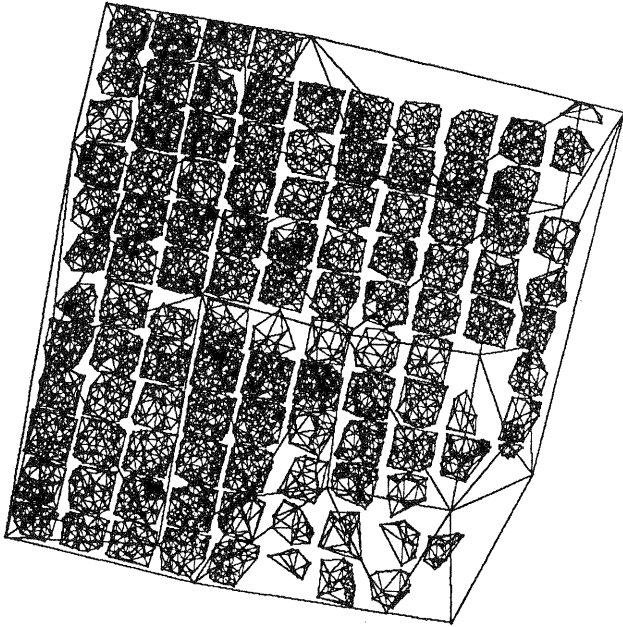


Figure 7: Derived combined subimage triangulations in ENH coordinates.

water bodies. The loss of information at the corners is due to the rotation between the stereo pairs with resultant loss of overlap as well as interference from clouds. The sparsity of points between subimages may be overcome by re-running the program with subimage centers shifted half a subimage width.

Any ENH file may be directly tested by manually observing the points on the stereoplotter. This provides accurate estimations of the RMS errors of the linear feature-based procedure. RSME values are currently between 10 and 20 meters with less than 10% incorrect matches (some subimage pairs contained no mismatches). However, visually examining the line pairs overlaid on the stereo images revealed that many mismatches involved features of opposite contrast, e.g. the edge of one side of a road matched the edge on the other side of the road in the other image. All line parameters were similar including the *absolute* value of the contrast.

It is suggested that instead of allowing the orientation angle to be measured on a resultant 180° scale, to measure it on 360° scale. Thereby, producing line vectors whose direction is dependent not only on their orientation but on their contrast as well. E.g. the vector always points in the direction where the higher intensity pixels are on its right.

Once this is done, the weights of the line pair parameters may possibly be optimized (changed from their current values) by performing gradient descent in the weight space. Steepest descent or gradient methods are characterized by iterative algorithms for improving estimates of control parameters. Some estimations are required during the iterative procedure to judge the extent of nonlinearity so that the linearized prediction will be reasonably accurate. This is done in the hope that the procedure shall converge on a "correct" solution given a set of line pairs, their similarity parameters and whether or not they match.

Failing this, at least determine which parameters contribute more to correct matches and which contribute more to the incorrect matches. This may allow the removal of most of the false matches without resorting to triangulating the points in ENH (UTM) coordinates and removing anomalous peaks and troughs.

A DEM of the region on a 250 meter grid interval has been previously obtained manually by visually analyzing the stereo images on an analytical stereoplotter. It is also possible to *drape* one intensity image of the stereo pair over the DEM to obtain a realistic impression of the original terrain. This allows comparison in 3D between a DEM which has been previously obtained manually and the derived DEM.

6 Conclusion

The method described of extracting and matching linear features from stereo satellite images has been implemented and has proved to be a reliable procedure for terrain generation with height accuracies approaching the pixel level.

The line extraction and matching techniques outlined have not only produced some good results visually, but have been tested on the stereoplotter. The extraction of straight lines from images produces a rich set of descriptive parameters, allowing a flexible algorithm to be implemented during matching. This method may also be applied in the near range (industrial applications, robot vision) with more emphasis placed on line-linking, as less features are involved and each has more importance.

It is an aim to incorporate this feature-based system with the area-based system which is already developed to a high standard. The two systems combined may prove to be a powerful tool and be highly complementary, especially as the area-based system is limited to the grid resolution it may achieve by the size of its correlation window. The feature-based system may then be called upon to provide additional points within this window. Alternatively, the features may be used in conjunction with the Moravec Operator to locate points of interest.

The method may be expanded upon, perhaps by performing parameter tuning in the weight space using parameter optimization techniques. Contextual analysis of features and the identification of features are seen as possible future avenues for this technique.

7 Acknowledgments

The author gratefully appreciates suggestions and encouragement from John Trinder. Thanks also go to Brian Donnelly for camera model equations and to Christophe Angleraud and Martin Dennis for assistance with graphics.

References

- [1] Ballard, D.H., C.M. Brown, 1982. Computer Vision. Englewood Cliffs, NJ: Prentice-Hall.
- [2] Barnard, S.T., M.A. Fishler, 1982. Computational Stereo. ACM Computing Surveys, 14, No. 4, 553-572.

- [3] Brockelbank, D.C., A. P. Tam, 1991. Stereo Elevation Determination Techniques for SPOT Imagery. *Photogrammetric Engineering and Remote Sensing*, 57, No. 8, 1065-1073.
- [4] Burns, J.B., A.R. Hanson, E.M. Riseman, 1986. Extracting Straight Lines. *PAMI-8*, No. 4, 425-455.
- [5] Greenfeld, J.S., A.F. Schenk, 1989. Experiments with Edge-Based Stereo Matching. *Photogrammetric Engineering and Remote Sensing*, 55, No. 12, 1771-1777.
- [6] Hannah, M.J., 1989. A System for Digital Stereo Image Matching. *Photogrammetric Engineering and Remote Sensing*, 55, No. 12, 1765-1770.
- [7] Kratky, V., 1989. On-Line Aspects of Stereophotogrammetric Processing of SPOT Images. *Photogrammetric Engineering and Remote Sensing*, 55, No. 3, 311-316.
- [8] McIntosh, J.H., K.M. Mutch, 1988. Matching Straight Lines. *Computer Vision, Graphics and Image Processing*, 43, 386-408.
- [9] Medioni G., R. Nevatia (1985) Segment-Based Stereo Matching. *Computer Vision, Graphics and Image Processing*, 31, 2-18.
- [10] Theodossiou, E.I., I.J. Dowman, 1990. Heighting Accuracy of SPOT. *Photogrammetric Engineering and Remote Sensing*, 56, No. 12, 1643-1649.
- [11] Trinder, J.C., B.E. Donnelly, K.L. Keong (1988), SPOT Mapping Software for Wild Aviolyt BC2 Analytical Plotter. *International Archives of Photogrammetry and Remote Sensing*, Vol. 27, Pt. B4, 412-421.
- [12] Winston, P.H., B.K.P. Horn, 1984. *Lisp*, Chap 10 - Examples Involving Arrays and Binary Images. Addison-Wesley.
- [13] Zhou, Y.T., V. Venkateswar, R. Chellappa, 1989. Edge Detection and Linear Feature Extraction Using a 2-D Random Field Model, *PAMI-11*, No. 1, 84-95.